

# Electromechanical properties of thin strip piezoelectric vibrators at high frequency

Timothy Ritter,<sup>a)</sup> K. Kirk Shung, Wenwu Cao, and Thomas R. Shrout

*NIH Resource Center for Medical Ultrasonic Transducer Technology, Penn State University, 205 Hallowell Building, University Park, Pennsylvania 16802*

(Received 8 March 2000; accepted for publication 3 April 2000)

A method was developed and used to determine the electromechanical properties of high frequency (>20 MHz) piezoelectric strip vibrators. A nonlinear regression technique was employed to fit the impedance magnitude and phase as predicted by Mason's model to measured values. Results from experimental measurements on 30 MHz array elements supported by an attenuative backing indicated degraded performance when compared to values predicted from the electromechanical properties measured at low frequency. This degradation may be attributed to damage incurred during fabrication and grain size effects, with a fine grain sized material providing superior relative performance. This technique may be used in the evaluation and comparison of different fabrication processes and materials for high frequency medical imaging arrays. © 2000 American Institute of Physics. [S0021-8979(00)05913-2]

## I. INTRODUCTION

Ultrasonic imaging at frequencies from 20 to 100 MHz can provide high spatial resolution for dermatological, ophthalmological, articular, and intravascular applications.<sup>1</sup> Current imaging systems in this frequency range rely on mechanically scanned single element transducers to interrogate the tissue of interest. For enhanced performance a solid-state array is desired, where multiple thin strip resonators are placed adjacently and are mechanically and electrically isolated. The small scale required of devices operating above 20 MHz, where individual elements are less than 100  $\mu\text{m}$  tall and 50  $\mu\text{m}$  wide, has severely limited the development of high frequency arrays. Fabrication techniques capable of achieving devices of this scale often alter the electromechanical properties due to physical damage and departures from the desired geometry. In addition, piezoelectric materials display frequency dispersion in most electromechanical properties.<sup>2</sup> It is therefore desirable to determine the properties of high frequency array elements after fabrication.

The resonance technique is often used for measuring the electromechanical properties at low frequencies, where it is practical to fabricate and test air-loaded resonators.<sup>3</sup> Above 20 MHz, the electrical interconnect and measurement of air loaded array elements is problematic due to the small device size. It is therefore desirable to support the element with a conductive substrate. Supported piezoelectric films have been characterized using a comparison of experimental electrical impedance data and an analytical solution of the one-dimensional wave equation.<sup>4</sup> This technique is not directly suited to high frequency array elements, however, due to coupling between the width and height resonances. A method for approximating the coupling between these resonances has also been described, but the procedure is cumbersome and does not lend itself to determining the full electromechanical properties.<sup>5</sup> A simplified method of analyzing the

elastic, piezoelectric, and dielectric properties of high frequency array elements supported by a substrate is proposed herein. This technique has been used to determine the properties of two commonly used polycrystalline piezoelectric materials when applied to a high frequency linear array design.

## II. CHARACTERIZATION METHOD

A popular method of predicting the performance of piezoelectric devices is to approximate them as one-dimensional vibrators and develop an equivalent circuit by application of network theory. The Mason equivalent circuit, shown in Fig. 1 for a one-dimensional thickness extensional vibrator, has been used extensively for modeling piezoelectric and transducer performance.<sup>6</sup> Other circuits such as the *KLM* model are also used extensively,<sup>7</sup> but since they are based on the same differential equations they differ only in form and reduce to the same solution.<sup>8</sup> For this work the Mason model was used to determine the electromechanical properties of a piezoelectric array element, as opposed to the traditional use of predicting electrical or acoustic performance based on previously measured properties.

Figure 2 shows the geometry of a representative 30 MHz linear array element. The  $z$  axis represents the direction of poling. The  $y$  axis is assumed to be effectively infinite and presents a boundary condition of zero strain ( $S$ ) near the height resonance. The boundary condition in the  $x$  direction is neither zero stress nor zero strain, but approaches a condition of zero stress ( $T$ ) as the ratio of height to width approaches infinity. The electromechanical properties applicable to this geometry, labeled with a prime ( $'$ ) according to the convention of DeSilets,<sup>9</sup> are  $c_{33}^{D'}$ ,  $k_{33}'$  and  $\epsilon_{33}^{S'}$ . It is helpful to write each of these properties as complex quantities (denoted with an  $*$ ) according to the following convention:<sup>10</sup>

$$c_{33}^{D'*} = c_{33}^{D'}(1 + i \tan \delta_m), \quad (1)$$

$$\epsilon_{33}^{S'*} = \epsilon_{33}^{S'}(1 - i \tan \delta_e), \quad (2)$$

$$k_{33}'^* = k_{33}'(1 + i \tan \delta_k). \quad (3)$$

<sup>a)</sup>Electronic mail: tar145@psu.edu

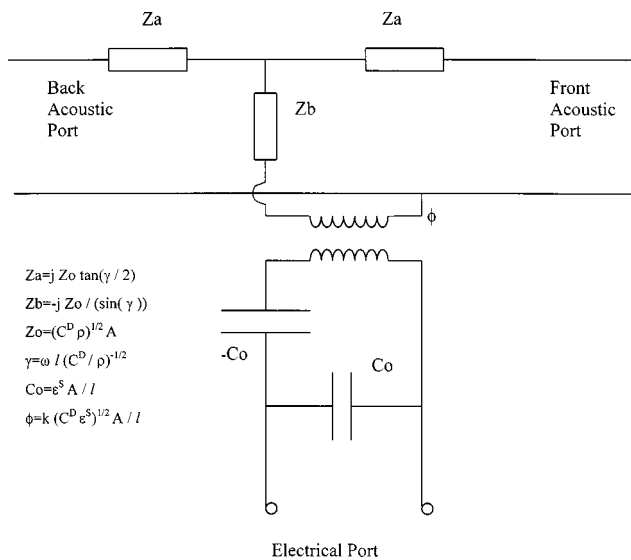


FIG. 1. Mason's model for a thickness-resonant device.  $k$  is the coupling coefficient,  $C^D$  is the elastic constant,  $\epsilon^S$  is the clamped permittivity,  $\rho$  is the density of the piezoelectric,  $A$  is the electroded area,  $l$  is the thickness, and  $\omega$  is the angular frequency. Additional loads on either acoustic port can be represented either by a  $T$  network for finite dimensions or by an impedance for infinite dimensions (see Ref. 6).

Given the geometry in Fig. 2 it is possible to determine the properties of an array element using the Mason model. The advantage of doing this is that the elements can be supported by a substrate (often referred to as a backing material) during measurement. The properties can then be extracted from the measured data using nonlinear regression to fit measured and modeled electrical impedance. It has previously been shown that one-dimensional models can provide an excellent approximation to the performance of backed array elements resonating in air as long as the ratio of width to height (aspect ratio) does not exceed 0.7.<sup>9,11</sup> In order to effectively approximate this multidimensional problem using a one-dimensional model it is important or point out the following limitations:

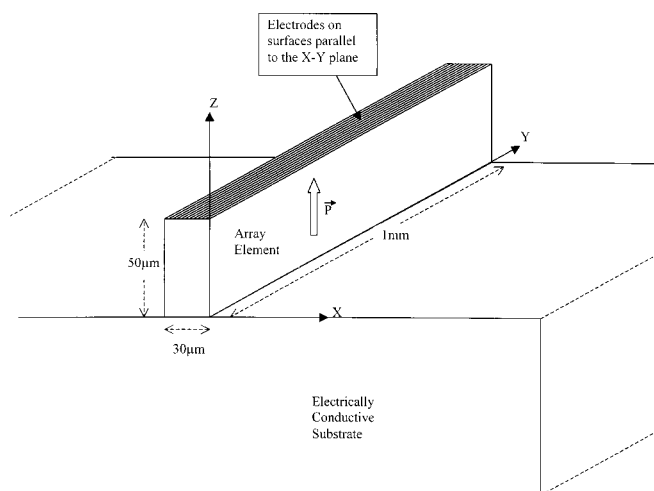


FIG. 2. The geometry of a representative element used in a 30 MHz linear array. The  $z$  axis represents the direction of poling, and electrodes are applied to the top and bottom faces.

(1) The backing must present a real and well-defined acoustic load. DeSilets<sup>9</sup> has shown that as long as the product of the wave number for a longitudinal plane wave and the width exceeds one, the effective load impedance is equal to the longitudinal plane wave impedance of the backing.

(2) The measured properties (especially the elastic constant) depend on the aspect ratio and cannot be generalized to other configurations. This limitation is true with air loaded resonators as well.

(3) Care must be taken to avoid acoustic interactions between elements if a multi-element array is tested. The use of a high attenuation backing is recommended, as is the use of a wide separation between the elements.

(4) The elements are often damaged during fabrication. For example, laser dicing can result in tapered element cross sections, thermal damage, and redeposited material, thereby changing the resonant behavior. One of the uses of the model, therefore, would be to assess the effects of the fabrication process.

Two different piezoelectric materials were fabricated using fine scale mechanical dicing: a fine grain size ( $< 2 \mu\text{m}$ ) PZT-5H equivalent material (TRS600FG, TRS Ceramics, Inc., State College, PA) and an ultrahigh permittivity material with a  $6.5 \mu\text{m}$  grain size (TRSHK1, TRS Ceramics, Inc., State College, PA). The material in the form of a thin plate was lapped to the desired thickness and backed with a highly attenuative silver-epoxy thermoset composite. The acoustic impedance of this backing was measured to be 5.92 MRayls at 30 MHz and the longitudinal attenuation was over 100 dB/mm. The elements were connected using a flexible circuit bonded across the face of a rigid frame. The backed piezoceramic was then bonded into a slot machined into the center of the assembly such that the interconnect traces extended beyond the frame on both sides. Sputtered Cr/Au was used to electrically connect the flexible circuit and the piezomaterial. The ends of the circuit were then folded out of the way and the elements were diced using a K&S model 982-6 dicing saw. After fabrication the piezoelectric elements were re-poled under an electric field of 30 kV/cm for 5 min at room temperature and aged for 24 h. Electrical measurements were obtained using an HP 4194 impedance analyzer using the Z-probe attachment.

The curve-fitting routine was implemented in Matlab using a Gauss-Newton algorithm to fit six variables:  $c_{33}^{D'}$ ,  $k_{33}'$ ,  $\epsilon_{33}^{S'}$ ,  $\tan \delta_m$ ,  $\tan \delta_e$ , and  $\tan \delta_k$ . The thickness of the sputtered gold was accounted for in the Mason model using a  $T$  network,<sup>6</sup> since the electrode mass loads the ceramic and shifts the resonant spectrum at high frequencies. The routine was implemented in two parts: (1) a fit to  $|Z|$  was used to obtain the variables  $c_{33}^{D'}$ ,  $k_{33}'$ ,  $\epsilon_{33}^{S'}$ ,  $\tan \delta_m$ , and  $\tan \delta_k$  and (2) a fit to the electrical phase angle was used to obtain  $\tan \delta_e$ , since the dielectric loss tangent is heavily dependent on the phase angle.<sup>10</sup> 120 data points were used in the range from 25 to 40 MHz, and three iterations of the program resulted in convergence for all cases. Figure 3 shows a block diagram describing the program.

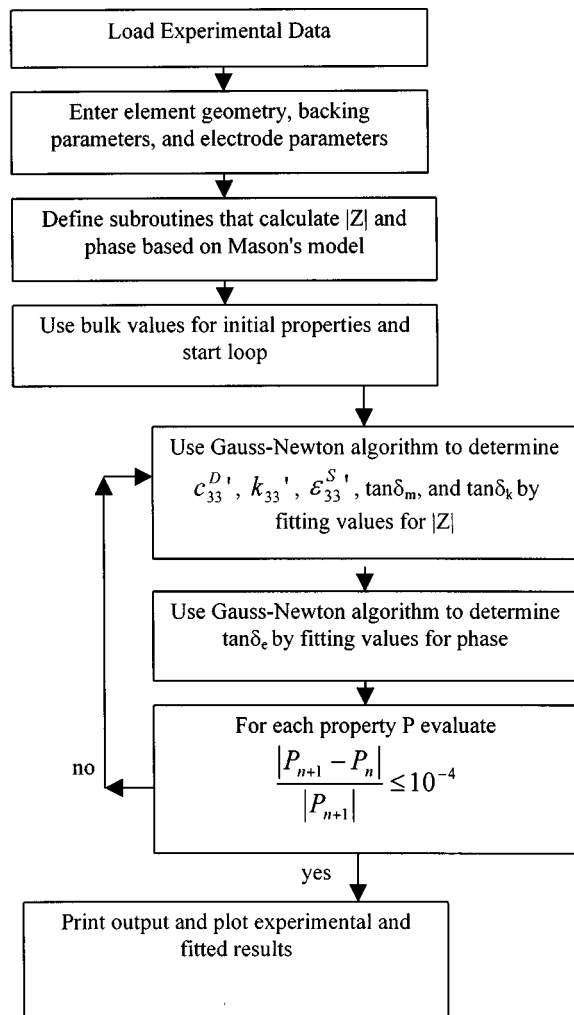


FIG. 3. A flow chart showing the algorithm used to determine the properties of array elements.

### III. RESULTS AND DISCUSSION

Array elements with nominal parallel resonance frequencies near 35 MHz were prepared, tested, and characterized as described earlier. Groups of three elements were tested simultaneously for each of the two materials, with physical separations of 100  $\mu\text{m}$  between the elements. A summary of the results is shown in Table I and an example of the fitted data is shown in Fig. 4.

Physical inspection of the elements after fabrication revealed visible chipping and grain pullout on the elements fabricated from TRSHK1, while damage to the TRS600FG material was minimal. This physical damage would be expected to correspond to a reduction in the effective dielectric permittivity and piezoelectric coupling. A comparison of the

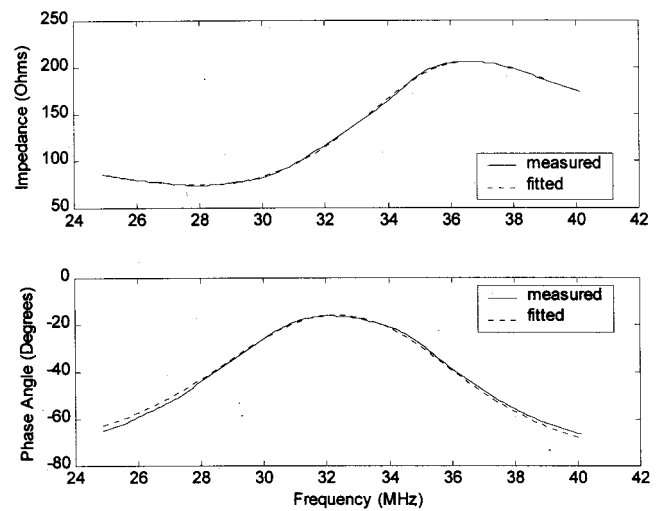


FIG. 4. The measured and curve-fitted impedance and phase angle spectra for the TRSHK1 material.

measured  $k'_{33}$  and  $\epsilon_{33}^{S'}$  to the values predicted from the bulk electromechanical properties reveals this effect. It is important to point out that the bulk properties were measured using air-loaded resonators at frequencies well below 10 MHz. The diced TRS600FG elements demonstrated  $k'_{33}$  and  $\epsilon_{33}^{S'}$  values that were 90% and 85% of the expected values, respectively. The TRSHK1 elements displayed a greater reduction in performance, with  $k'_{33}$  and  $\epsilon_{33}^{S'}$  values that were only 80% and 70% of the predicted values. Thickness coupling in thin plates has been shown to degrade at a rate of 0.6%–2% per decade of frequency above 20 MHz.<sup>12</sup> A similar effect occurring for array elements would account for only a small fraction of the degradation observed. The degree of physical damage may therefore be determined from the measured properties. In addition, the difficulty in fabrication and the increased  $\tan \delta_m$  evident for the TRSHK1 may be a result of the large grain size.<sup>12</sup> This indicates that the TR600FG is preferred for high frequency applications.

### IV. CONCLUSIONS

A method of measuring the properties of high frequency piezoelectric strip vibrators based on the Mason model has been presented. Both the substrate supporting the elements and the width of the elements must be properly selected when implementing this method. Measurements on two piezoelectric materials, fabricated using mechanical dicing, indicated degraded performance when compared to values predicted from the bulk electromechanical properties. These reductions may be attributed to damage that occurred during

TABLE I. Properties of supported array elements measured by curve-fitting experimental impedance data to the Mason model. Values for  $k'_{33}$  and  $\epsilon_{33}^{S'}/\epsilon_0$  determined from bulk electromechanical properties are also listed for comparison.

Material	Height (mm)	Width (mm)	$c_{33}^{D'}$ (N/m <sup>2</sup> )	$k'_{33}$	$k'_{33}$ (bulk)	$\epsilon_{33}^{S'}/\epsilon_0$	$\epsilon_{33}^{S'}/\epsilon_0$ (bulk)	$\tan \delta_k$	$\tan \delta_m$	$\tan \delta_e$
TRS600	0.050	0.029	$10.9 \times 10^{10}$	0.62	0.69	1290	1500	-0.03	0.01	0.03
TRSHK1	0.052	0.028	$11.4 \times 10^{10}$	0.56	0.68	1950	2900	-0.05	0.09	0.04

fabrication and to grain size effects, with the fine grain material providing superior relative performance. The technique presented here may be used in the evaluation and comparison of different fabrication processes and materials for high frequency array applications.

#### ACKNOWLEDGMENT

Financial support for this work was provided through NIH Grant No. P41-RR11795.

<sup>1</sup>G. R. Lockwood, D. H. Turnbull, D. A. Christopher, and F. S. Foster, *IEEE Eng. Med. Biol. Mag.* **15**, 60 (1996).

<sup>2</sup>H. Wang, W. Jiang, and W. Cao, *J. Appl. Phys.* **85**, 8083 (1999).

<sup>3</sup>IEEE Std. 176-1987 (IEEE, New York, 1987).

<sup>4</sup>M. Lukacs, T. Olding, M. Sayer, R. Tasker, and S. Sherrit, *J. Appl. Phys.* **85**, 2835 (1999).

<sup>5</sup>M. Onoe and H. F. Tiersten, *IEEE Trans. Ultrasonics Eng.* **10**, 32 (1963).

<sup>6</sup>P. D. Edmonds, *Ultrasonics*, Methods of Experimental Physics Vol. 19 (Academic, New York, 1981).

<sup>7</sup>R. Krimholtz, D. A. Leedom, and G. L. Matthaei, *Electron. Lett.* **6**, 398 (1970).

<sup>8</sup>S. Sherrit, S. Leary, B. Dolgin, and Y. Bar-Cohen, *Proc. IEEE Ultr. Symp.*, Lake Tahoe, NV, October, 1999 (in press).

<sup>9</sup>C. S. DeSilets, Ph.D. thesis, Stanford (Edward L. Ginzton Laboratory, Stanford, 1978).

<sup>10</sup>K. W. Kwok, H. L. W. Chan, and C. L. Choy, *IEEE Trans. Ultrason. Ferroelectr. Freq. Control* **44**, 733 (1997).

<sup>11</sup>A. R. Selfridge, Ph.D. thesis, Stanford (Edward L. Ginzton Laboratory, Stanford, 1982).

<sup>12</sup>M. J. Zipparo, K. K. Shung, and T. R. Shrout, *IEEE Trans. Ultrason. Ferroelectr. Freq. Control* **44**, 1038 (1997).